Preprints of the 19th World Congress
The International Federation of Automatic Control
Cape Town, South Africa. August 24-29, 2014

Controlled synchronization: a Huygens' inspired approach ⋆

J. Pena Ramirez * **A. Denasi** ** **A. Rodriguez-Angeles** ***,** **J. Alvarez Gallegos** **** **H. Nijmeijer** **,† **K. Aihara** *,‡

* *Collaborative Research Center for Innovative Mathematical Modelling, Institute of Industrial Science, The University of Tokyo, 4-6-1 Komaba, Meguro-ku, Tokyo 153-8505, Japan (email: jpena@sat.t.u-tokyo.ac.jp)*
** *Eindhoven University of Technology, P.O. Box 513 5600 MB Eindhoven, The Netherlands (email: A.Denasi@tue.nl)*
*** *Research Center for Advanced Studies (Cinvestav-IPN), Mechatronics Group, Mexico, D.F. (email: aangeles@cinvestav.mx)*
**** *Center for Scientific Research and Higher Education at Ensenada, Mexico (CICESE), Carretera Ensenada-Tijuana No. 3918, Zona Playitas, C.P. 22860, Ensenada, B.C. Mexico. (e-mail: jqalvar@cicese.mx)*
† *(email: H.Nijmeijer@tue.nl)*
‡ *(email: aihara@sat.t.u-tokyo.ac.jp)*

Abstract: This paper considers synchronization as a control problem. In particular, a (robust) controller for achieving synchronization in pairs of second order nonlinear systems is designed. The design is inspired by the classical experiment on synchronization of pendulum clocks, as described by Christiaan Huygens. In the proposed control scheme, the systems do not interact directly but through an exogenous system. Ultimately, it is demonstrated that Huygens' controller, can be used to perform in-phase and anti-phase synchronized tasks, with the advantage that 'small' control gains are required. The stability of the closed-loop system is analyzed using perturbation theory and the proposed controller is experimentally validated on a pair of Cartesian robots.

Keywords: Controlled synchronization, Huygens' controller, perturbation theory, second order systems, robust control, control applications.

1. INTRODUCTION

In general, synchronization is understood as the phenomenon that keeps things "happening at the same time". There exists a more exquisite definition of synchronization due to Christiaan Huygens, a Dutch scientist who around 1665 discovered that a pair of pendulum clocks, placed on a flexible structure, exhibited synchronized motion due to the imperceptible vibrations of the coupling structure. Huygens referred to this phenomenon as the *sympathy* of two clocks (Huygens, 1660).

In the words of Huygens, it can be said that we live in a sympathetic world. For example, frogs make alternated mating calls, neurons and pacemaker cells fire in unison, and many other examples that are perceptible to everyone. Some of these examples have attracted the interest of specialists in diverse disciplines ranging from physics to mathematics passing through neuroscience and control. Their objective is to understand the phenomenon and then to find scientific and technological applications. See e.g., Hoppensteadt and Izhikevich (2001); Aihara et al. (2008); Wang et al. (2011); Nijmeijer (2001).

The purpose of this paper is to address the synchronization phenomenon from a control perspective. A feedback controller for achieving synchronization of two arbitrary second order nonlinear systems is designed. It is inspired by Huygens' classical experiment on synchronization of pendulum clocks. The ultimate aim of the controller is to synchronize (either in phase or in anti-phase) two second order nonlinear systems with respect to a desired trajectory.

First, we design the controller by assuming the following ideal conditions: complete knowledge of the system dynamics and availability of the complete state vector. Then, the resulting closed-loop system is analyzed by using a perturbation method. The analysis provides analytic expressions for choosing the gains of the proposed controller such that the resulting closed-loop system is stable and control towards in-phase or anti-phase synchronization is achieved. Next, a robust version of the aforementioned controller is derived by inserting a robust differentiator

⋆ This work was partly supported by the CONACyT under Grant CB2012-180011-Y and by the Aihara Innovative Mathematical Modelling Project, the Japan Society for the Promotion of Science (JSPS) through the "Funding Program for World-Leading Innovative R&D on Science and Technology (FIRST Program)," initiated by the Council for Science and Technology Policy (CSTP).

in the loop, which provides robustness against unmodelled dynamics and parameter uncertainties. The analytic results are supported by means of experiments on two Cartesian robots—a physical robot and a 'virtual' robot. Ultimately, it is demonstrated that the coupling used by Huygens to synchronize his pendulum clocks can be transformed into a controller for synchronization tasks of arbitrary second order nonlinear systems.

The proposed control scheme provides an alternative for the well-known master-slave and mutual synchronization schemes, cf. (Nijmeijer and Rodriguez-Angeles, 2003). One of the differences of our controller regarding current approaches is that the interaction between the systems to synchronize is indirect and 'weak'. Furthermore, in closed-loop the systems behave as self-sustained oscillators interacting via dynamic coupling. The required coupling signal to achieve synchronization is 'small' and it vanishes when the systems are completely synchronized.

The outline of the paper is as follows. Section 2 presents the controlled synchronization problem. In Section 3 the Huygens controller is introduced and the main theoretical results are derived. Next, a robust version of Huygen's controller is proposed in Section 4. Then, in Section 5, the controller is experimentally validated. Finally, a discussion of the results is included in Section 6.

2. CONTROLLED SYNCHRONIZATION PROBLEM

The original experiment on synchronization, as described by Huygens in his lab notebook, consists of two pendulum clocks mounted on a wooden bar resting on top of two chairs (see Huygens (1660) for a picture). The coupled system shows at least two possible limit behaviours: in-phase and anti-phase synchronized motion of the pendula. Some particular characteristics of the Huygens system are: the interaction between the clocks is not direct but through the wooden bar, to which they are attached. Moreover, when the pendula of the clocks are synchronized in anti-phase, the coupling bar comes to standstill (in the ideal case, i.e. identical pendula). Hence, in the limit, the clocks run uncoupled but synchronized. Another feature of the Huygens system is that the coupling strength, i.e. the parameter that determines how weak or strong the interaction is between the clocks, is 'small'.

In this manuscript, we consider Huygens' synchronization problem from a control point of view. Instead of pendulum clocks we consider arbitrary second order nonlinear systems and the coupling bar is replaced by a suitable controller, such that the closed-loop system resembles the original Huygens' system, as depicted in Figure 1.

We consider systems of the form:

$$\ddot{x}_j = f_j(x_j, \dot{x}_j) + u_j, \quad \text{for} \quad j = 1, 2, \tag{1}$$

where $x_j, \dot{x}_j \in \mathbb{R}$ is the state, $f_j(x_j, \dot{x}_j)$ is a nonlinear function, and $u_j \in \mathbb{R}$ is a control input.

The problem considered in the paper is to design a suitable control input of the form:

$$u_j = G(x_j, \dot{x}_j, z, q_r(t)), \quad \text{for} \quad j = 1, 2, \tag{2}$$

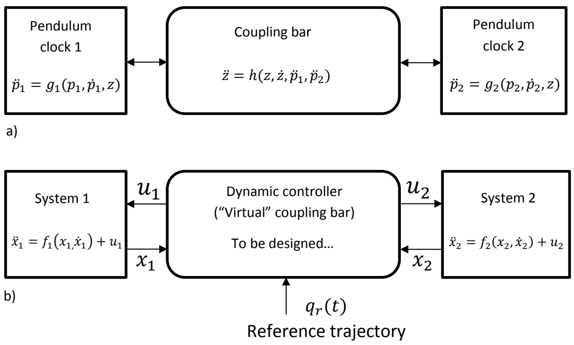

Fig. 1. a) Original Huygens' synchronization scheme. b) Proposed control scheme inspired by Huygens' scheme. The clocks are replaced by arbitrary second order nonlinear systems and the coupling bar is replaced by a suitable controller, such that the closed-loop has the synchronization properties of Huygens' system and, moreover, synchronization with respect to the reference trajectory $q_r(t)$ is achieved.

where $q_r(t)$ is a given desired trajectory and $z \in \mathbb{R}$ is the coupling variable, which is generated by a dynamical system of the form

$$\ddot{z} = h(z, \dot{z}, x_1, \dot{x}_1, x_2, \dot{x}_2, \ddot{q}_r), \tag{3}$$

such that systems (1) asymptotically synchronize with respect to the desired trajectory $q_r(t)$, i.e.

$$\lim_{t\to\infty} (x_1(t) \mp q_r(t)) = 0, \qquad \lim_{t\to\infty} (x_2(t) - q_r(t)) = 0, \tag{4}$$

and the interaction between the synchronized systems disappears, i.e.

$$\lim_{t\to\infty} z(t) = 0. \tag{5}$$

The $\mp$ sign in (4) indicates that the proposed controller (2) can be used to solve either the in-phase or the anti-phase synchronization problems: $-$ for in-phase and $+$ for anti-phase.

3. CONTROLLED SYNCHRONIZATION OF ARBITRARY SECOND ORDER NONLINEAR SYSTEMS

In this section, we propose a novel controller for synchronizing two nonlinear systems of the form

$$\frac{\mathrm{d}}{\mathrm{d}t}\begin{bmatrix} x_{1j} \\ x_{2j} \end{bmatrix} = \begin{bmatrix} x_{2j} \\ f_j(x_{1j}, x_{2j}) \end{bmatrix} + \begin{bmatrix} 0 \\ 1 \end{bmatrix} u_j, \tag{6}$$

where $x_{1j}, x_{2j} \in \mathbb{R}$ are the state variables, $f_j(x_{1j}, x_{2j})$ is a nonlinear function, and $u_j \in \mathbb{R}$ is a control input, for $j = 1, 2$.

The control objective is as formulated in (4), i.e. to synchronize the systems, either in-phase or in anti-phase, with respect to a given *periodic* and *smooth* reference trajectory $q_r(t)$. Here, we consider trajectories of the form

$$q_r(t) = a \sin \omega t, \tag{7}$$

where $a \in \mathbb{R}_+$ and $\omega \in \mathbb{R}_+$ determine the amplitude and frequency of the reference trajectory, respectively.

First, we consider the case of controlled in-phase synchronization. Then, we extend the obtained results to the case of controlled anti-phase synchronization.

3.1 Controlled in-phase synchronization

The proposed control inputs for (6) are given by

$$u_j = -f_j(x_{1j}, x_{2j}) - \omega^2 (x_{1j} + z) - \mu c(H_j - H^*) x_{2j} \\ -\mu(k_p e_j + k_v \dot{e}_j), \qquad \text{for } \ j = 1, 2, \tag{8}$$

where $\omega \in \mathbb{R}_+$, is the frequency of the reference trajectory, μ is a small parameter, i.e. $0 < \mu << 1$, which determines the coupling strength between the systems, the variables $e_j = x_{1j} - q_r$ and $\dot{e}_j = x_{2j} - \dot{q}_r$ denote the tracking errors, $k_p, k_v \in \mathbb{R}_+$ are gains to be designed, and

$$H_j = x_{2j}^2 + x_{1j}^2, \qquad H^* = \dot{q}_r^2(t) + q_r^2(t), \tag{9}$$

where $q_r(t)$ is the reference trajectory as given in (7) and $\dot{q}_r(t)$ denotes the time derivative of the reference (compare to (Pena-Ramirez et al., 2013)).

The variable z in (8), which we refer to as Huygens' coupling, is generated by the dynamical system

$$\ddot{z} = -\omega^2 z - s\dot{z} + \mu \sum_{j=1}^{2} \left[\omega^2 (x_{1j} + z) + \mu c(H_j - H^*) x_{2j}\right] \\ +2\mu \ddot{q}_r(t), \tag{10}$$

where $s \in \mathbb{R}_+$ and $\ddot{q}_r(t)$ is the second time derivative of the reference signal $q_r(t)$ given in (7).

By defining the state vector $x = [x_{11}\ x_{21}\ x_{12}\ x_{22}\ z\ \dot{z}]^T$, the closed-loop (6),(8-10) takes the form

$$\dot{x} = \underbrace{\begin{bmatrix} 0 & 1 & 0 & 0 & 0 & 0 \\ -\omega^2 & 0 & 0 & 0 & -\omega^2 & 0 \\ 0 & 0 & 0 & 1 & 0 & 0 \\ 0 & 0 & -\omega^2 & 0 & -\omega^2 & 0 \\ 0 & 0 & 0 & 0 & 0 & 1 \\ 0 & 0 & 0 & 0 & -\omega^2 & -s \end{bmatrix}}_{A} x + \mu \underbrace{\begin{bmatrix} 0 \\ \Gamma_1 \\ 0 \\ \Gamma_2 \\ 0 \\ \Gamma_3 \end{bmatrix}}_{F(x,t)}, \tag{11}$$

where $\Gamma_1 = -c(x_{11}^2 + x_{21}^2 - q_r^2 - \dot{q}_r^2)x_{21} - k_p e_1 - k_v \dot{e}_1$, $\Gamma_2 = -c(x_{12}^2 + x_{22}^2 - q_r^2 - \dot{q}_r^2)x_{22} - k_p e_2 - k_v \dot{e}_2$, and $\Gamma_3 = \sum_{j=1}^{2} \left(\omega^2 (x_{1j} + z) + \mu c(H_j - H^*) x_{2j}\right) + 2\ddot{q}_r(t)$. Moreover, by using the transformation $x = Vy$, where V is the matrix of eigenvectors associated to matrix A in (11) and $y = [y_1, \ldots, y_6]^T$, the system can be diagonalized to

$$\dot{y} = Dy + \mu V^{-1} F(Vy, t), \tag{12}$$

where $D = \text{diag}(\omega i, -\omega i, \omega i, -\omega i, r_1, r_2)$, $i = \sqrt{-1}$, $r_1 = -\frac{1}{2}\left(s - \sqrt{s^2 - 4\omega^2}\right)$, and $r_2 = -\frac{1}{2}\left(s + \sqrt{s^2 - 4\omega^2}\right)$.

Next, system (12) is analyzed using the mathematical framework described in the Appendix, which is based on the Poincaré method of perturbations.

The analysis starts by considering system (12) with $\mu = 0$. It is easy to show that in this case, (12) has the solutions:

$$y_1 = \alpha_1 e^{i\omega t}, \quad y_2 = \alpha_2 e^{-i\omega t}, \quad y_3 = \alpha_3 e^{i\omega t}, \quad y_4 = \alpha_4 e^{-i\omega t}, \\ y_5 = \alpha_5 e^{r_1 t}, \quad y_6 = \alpha_6 e^{r_2 t}. \tag{13}$$

The next step is to determine the values of α_k, for $k = 1, \ldots, 6$, such that the periodic solutions of (11) asymptotically reduce, for $\mu = 0$ to (13). Note, however, that y_5 and y_6 decay asymptotically. Hence, in the sequel we focus on the case $\alpha_5 = \alpha_6 \equiv 0$. Moreover, in order to have real solutions, it is necessary that $\alpha_1 = \alpha_2$ and $\alpha_3 = \alpha_4$. This can be easily shown by replacing (13) in the transformation $x = Vy$ used above. Hence, we are looking for periodic solutions of (11) in the form

$$x_{11}(t) = 2\frac{\alpha_1}{\omega} \sin \omega t, \qquad x_{21}(t) = 2\alpha_1 \cos \omega t, \tag{14}$$

$$x_{12}(t) = 2\frac{\alpha_3}{\omega} \sin \omega t, \qquad x_{22}(t) = 2\alpha_3 \cos \omega t. \tag{15}$$

By using Theorem 3 in the Appendix, it is possible to obtain the values of α_1 and α_3. Writting conditions (A.5) in terms of α_1, α_3 yields

$$P_1 = P_2 = \frac{\left(\frac{\omega a}{2} - \alpha_1\right)}{\omega^3} \left(c\alpha_1 \left(3\omega^2 + 1\right)\left(\frac{\omega a}{2} - \alpha_1\right) + \omega^2 k_v \right. \\ \left. -i\omega k_p\right) + \frac{\omega}{s}\left(\alpha_1 - \omega a + \alpha_3\right) = 0, \tag{16}$$

$$P_3 = P_4 = \frac{\left(\frac{\omega a}{2} - \alpha_3\right)}{\omega^3} \left(c\alpha_3 \left(3\omega^2 + 1\right)\left(\frac{\omega a}{2} - \alpha_3\right) + \omega^2 k_v \right. \\ \left. -i\omega k_p\right) \quad + \frac{\omega}{s}\left(\alpha_1 - \omega a + \alpha_3\right) = 0. \tag{17}$$

Straightforward computations show that the left-hand side of (16), (17) is satisfied if

$$\alpha_1 = \frac{\omega a}{2}, \qquad \alpha_3 = \alpha_1 = \frac{\omega a}{2}. \tag{18}$$

Thus, by using (18), the periodic solutions (14), (15) of system (11) are

$$x_{11}(t) = x_{12}(t) = q_r(t), \qquad x_{21}(t) = x_{22}(t) = \dot{q}_r(t). \tag{19}$$

Clearly, (19) reflects the fact that the oscillators synchronizes in-phase with respect to the reference trajectory $q_r(t)$.

It follows from Theorem 3 that the stability of these solutions can be determined by looking at the roots of the characteristic equation

$$p(\lambda) = \left[4\omega^4\lambda^2 + 8\omega^3\left(a^2 c\omega^2 + k_v\right)\lambda + g_1\right]\left[4s^2\omega^4\lambda^2 \right. \\ \left. + 8\omega^3\left(a^2 c s^2 \omega^2 + k_v s^2 - 2s\omega^2\right)\lambda + g_2\right], \tag{20}$$

where

$$g_1 = 3a^4c^2\omega^6 + 4k_p^2 + \left(8a^2ck_v - 2a^4c^2\right)\omega^4 + \left(4k_v^2 - a^4c^2\right)\omega^2, \\ g_2 = \left(3a^4c^2s^2 + 16\right)\omega^6 + \left(8a^2ck_v - 2a^4c^2\right)s^2\omega^4 \\ + \left(4k_v^2 - a^4c^2\right)s^2\omega^2 + 4s\left(k_p^2 s - 4a^2c\omega^6 - 4k_v\omega^4\right). \tag{21}$$

It can be shown that the roots of (20) have negative real parts if

$$k_v > \max\left\{\frac{a^2c}{2}, \frac{2\omega^2}{s}\right\}, \qquad k_p > 2\omega^2\sqrt{\frac{a^2c\omega^2 + k_v}{s}}. \tag{22}$$

The analytic results above can be summarized in the following result.

Theorem 1 (In-phase synchronization). *Consider the pair of systems (6). Suppose that the state of each system is available for measurement. Then, for a given reference* *trajectory $q_r(t) = a \sin \omega t$, with $a, \omega \in \mathbb{R}_+$, the Huygens controller (8)-(10) with $0 < \mu << 1$, $c, s \in \mathbb{R}_+$ and*

$$k_v > \max \left\{ \frac{a^2 c}{2}, \frac{2\omega^2}{s} \right\}, \qquad k_p > 2\omega^2 \sqrt{\frac{a^2 c \omega^2 + k_v}{s}}, \quad (23)$$

guarantees that the solutions of the closed-loop system (6),(8-10), asymptotically synchronize, with respect to the reference trajectory $q_r(t)$, as follows:

$$\begin{aligned} &\lim_{t \longrightarrow \infty} x_{11}(t) = x_{12}(t) = q_r(t), \quad \lim_{t \longrightarrow \infty} x_{21}(t) = x_{22}(t) = \dot{q}_r(t), \\ &\lim_{t \longrightarrow \infty} z(t) = \dot{z}(t) = 0, \end{aligned} \quad (24)$$

i.e. in the limit, synchronized tracking of the reference trajectory $q_r(t)$ is achieved and the systems 'run' uncoupled.

3.2 Anti-phase synchronization

As mentioned in the introductory section, Christiaan Huygens was able to observe anti-phase synchronization in his setup of pendulum clocks, i.e. the pendula of the clocks were oscillating in opposite directions. The proposed controller, which is inspired by the Huygens system, can also be used to solve the problem of controlled anti-phase synchronization.

In this case, the proposed control inputs, to synchronize systems (6), are given by

$$\begin{aligned} u_j = &-f_j(x_{1j}, x_{2j}) - \omega^2 \Delta_j(x_{ij}, z) - \mu c(H_j - H^*) x_{2j} \\ &-\mu(k_p e_j + k_v \dot{e}_j), \text{for} \quad i = 1, 2, \end{aligned} \quad (25)$$

where all parameters are as defined in previous subsection, $\Delta_1(x_{1j}, z) = (x_{11} - z)$, $\Delta_2(x_{12}, z) = (x_{12} + z)$, H and H^* are as given in (9), the variables $e_1 = x_{11} + q_r$, $\dot{e}_1 = x_{21} + \dot{q}_r$, $e_2 = x_{12} - q_r$, and $\dot{e}_2 = x_{22} - \dot{q}_r$ denote the tracking errors, $k_p, k_v \in \mathbb{R}_+$ are gains to be designed, and the variable z, i.e. Huygens' coupling, is generated by the dynamical system

$$\begin{aligned} \ddot{z} = &-\omega^2 z - s\dot{z} + \mu \left[\omega^2 \Delta_1(x_{1j}, z) + \mu c(H_1 - H^*) x_{21} \right] \\ &-\mu \left[\omega^2 \Delta_2(x_{12}, z) + \mu c(H_2 - H^*) x_{22} \right] - 2\mu \ddot{q}_r. \end{aligned} \quad (26)$$

By following the same procedure as used for the in-phase case, it is possible to derive the next result for controlled anti-phase synchronization:

Theorem 2 (**Anti-phase synchronization**). *Consider the pair of systems (6). Suppose that the state of each system is available for measurement. Then, for a given reference trajectory $q_r(t) = a \sin \omega t$, with $a, \omega \in \mathbb{R}_+$, the Huygens controller (25)-(26) with $0 < \mu << 1$, $c, s \in \mathbb{R}_+$ and*

$$k_v > \frac{a^2 c}{2}, \qquad k_p > 0, \quad (27)$$

guarantees that the solutions of the closed-loop system (6),(25),(26), asymptotically synchronize, with respect to the reference trajectory $q_r(t)$, as follows:

$$\begin{aligned} &\lim_{t \longrightarrow \infty} x_{11}(t) = -x_{12}(t) = -q_r(t), \\ &\lim_{t \longrightarrow \infty} x_{21}(t) = -x_{22}(t) = -\dot{q}_r(t), \\ &\lim_{t \longrightarrow \infty} z(t) = \dot{z}(t) = 0, \end{aligned} \quad (28)$$

i.e. in the limit, the systems 'run' uncoupled but synchronized in anti-phase: system 1 is synchronized in anti-phase with the reference trajectory and system 2 is synchronized in in-phase with the reference trajectory.

4. ROBUST CONTROLLED SYNCHRONIZATION OF TWO SYSTEMS

Note that the Huygens controllers (8),(10) (for in-phase synchronization) or (25),(26) (for anti-phase synchronization) require complete knowledge of the system dynamics and also require that the full state vector is available for measure. This is certainly a limitation, because such an ideal setting is impossible to find in real life systems.

In order to circumvent this problem, for each system (6), we use a high-order sliding modes (HOSM) differentiator derived by Levant (2003), which provides robust estimation of the state vector, and moreover, it is also used to estimate the original dynamics $f_j(x_{ij}, x_{2j})$ of system (6). We assume that only the state variable x_{1j} in (6) is measured. Each HOSM differentiator is given by

$$\begin{aligned} \dot{h}_{0j} &= \nu_{0j} = -\lambda_k L^{1/(k+1)} \text{sig}(h_{0j} - x_{1j})^{k/(k+1)} + h_{1j}, \\ \dot{h}_{1j} &= \nu_{1j} = -\lambda_{k-1} L^{1/k} \text{sig}(h_{1j} - \nu_{0j})^{(k-1)/k} + h_2 + u_j, \\ &\vdots \quad \cdots \\ \dot{h}_{(k-1)j} &= \nu_{(k-1)j} = -\lambda_1 L^{1/2} \text{sig}(h_{(k-1)j} - \nu_{(k-2)j})^{1/2} + h_k, \\ \dot{h}_{kj} &= -\lambda_0 L \text{sign}(h_{kj} - \nu_{(k-1)j}), \end{aligned} \quad (29)$$

where $k = 1, \ldots 5$, x_{1j} and u_j, for $j = 1, 2$, are the measured state and control input of system (6), respectively and $\text{sig}(w)^\gamma = |w|^\gamma \, \text{sign}(w)$. By a proper choice of parameters $\lambda_0, \ldots, \lambda_k$, and assuming that there is no measurement noise in the system, the following is guaranteed after a finite time transient (Levant, 2003):

$$h_{0j} = x_{1j}, \; h_{1j} = x_{2j}, \; h_{2j} = f_j(x_{1j}, x_{2j}), \text{ for } j = 1, 2. \quad (30)$$

Hence, a robust version of the Huygens controller (8), (10) for achieving controlled in-phase synchronization is obtained by replacing x_{2j} and $f_j(x_{1j}, x_{2j})$ by h_{1j} and h_{2j}, respectively. Similarly, a robust version of the anti-phase Huygens' controller can be obtained by replacing the aforementionated variables in (25) and (26).

5. EXPERIMENTAL VALIDATION

In this section, the designed Huygens' controller is experimentally validated. Two Cartesian robots are used for the experiments: a physical robot and a 'virtual' robot. The physical robot [1] is depicted in Figure 2, whereas the 'virtual' robot is software implemented. Although each robot has 4 degrees of freedom (dofs), in this study only two dofs are controlled, namely the translational and rotational motions of the robot. For the time being, only controlled in-phase synchronization is considered.

The dynamic model of the robots is given by (cf. Nijmeijer and Rodriguez-Angeles (2003)):

$$M\ddot{q}_j + F(\dot{q}_j) + \psi_j(q_j, \dot{q}_j, t) = \tau_j, \qquad \text{for} \quad j = 1, 2, \quad (31)$$

where subindex $j = 1$ denotes the real robot and subindex $j = 2$ denotes the virtual robot. The state vector of

[1] See Nijmeijer and Rodriguez-Angeles (2003) for details about this robot.

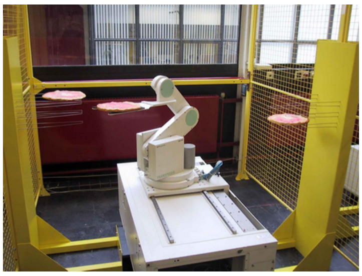

Fig. 2. Cartesian robot at TU/e.

robot j is given by $q_j = [q_{1j} \ q_{2j}]^T$, in which $q_{1j} \in \mathbb{R}$ denotes the translational dof and $q_{2j} \in \mathbb{R}$ corresponds to the rotational dof of robot j. The vector of applied torques is denoted by $\tau_j = [\tau_{1j} \ \tau_{2j}]^T$, $M \in \mathbb{R}^{2\times 2}$is the inertia matrix, and the term $\psi_j(q_{1j}, \dot{q}_{2j}, t) := [\gamma_{1j} \ \gamma_{2j}]^T$ contains unmodelled dynamics, parameter uncertainties, and possible bounded external disturbances. Moreover, if there are coupling terms between the dofs, these terms are also included in $\psi_j(\cdot)$. Finally, $F(\dot{q}_j) := [\bar{f}_{1j} \ \bar{f}_{2j}]^T$ denotes the vector of friction forces.

The state vector of the robots is reconstructed by using the HOSM differentiator (29). Note that for each robot, a pair of HOSM differentiators is necessary, one for each dof. Following Levant (2003), the parameter values for the HOSM differentiators are chosen as follows: $\lambda_0 = 1.1$, $\lambda_1 = 1.5$, $\lambda_2 = 3$, $\lambda_3 = 5$, $\lambda_4 = 8$, and $\lambda_5 = 12$.

Then, by using the results presented in Sections 3 and 4, the control inputs to the robots, which are also applied to the differentiators, are defined as follows:

$$\begin{bmatrix} \tau_{1j} \\ \tau_{2j} \end{bmatrix} = -M^{-1} \begin{bmatrix} h_{2q_{1j}} + \omega^2(q_{1j} + z) + \mu_1 c_1 \left(k_{p1} e_{1j} + k_{v1} \dot{e}_{1j}\right) \\ h_{2q_{2j}} + \omega^2(q_{2j} + z) + \mu_2 c_2 \left(k_{p2} e_{2j} + k_{v2} \dot{e}_{2j}\right) \end{bmatrix}$$
$$+ \begin{matrix} \mu_1 c_1 \left(h^2_{1q_{1j}} + q^2_{1j} - \dot{q}^2_{r1} - q^2_{r1}\right) h_{1q_{1j}} \\ \mu_2 c_2 \left(h^2_{2q_{2j}} + q^2_{2j} - \dot{q}^2_{r2} - \dot{q}_{r2}\right) h_{1q_{2j}} \end{matrix} \Bigg], \quad (32)$$

where $e_{1j} = q_{1j} - q_{r1}$, $\dot{e}_{1j} = h_1 q_{1j} - \dot{q}_{r1}$, $e_{2j} = q_{2j} - q_{r2}$, and $\dot{e}_{2j} = h_1 q_{2j} - \dot{q}_{r2}$, and the coupling variables z_j, i.e. the Huygens couplings, are generated by

$$\ddot{z}_j = -\omega^2 z_j - s\dot{z}_j + \mu_j \sum_{l=1}^{2} \left[\omega^2 \left(q_{1l} + z\right)\right.$$
$$\left. + \mu_j c_j (h^2_{1q_{1l}} + q^2_{1l} - q^2_{rj} - \dot{q}^2_{rj}) h_{1q_{1l}}\right] + 2\mu_j \ddot{q}_{rj}, (33)$$

for $j = 1, 2$, $l = 1, 2$. For this experiment, the following reference trajectories are considered:

$$q_{r1}(t) = 0.1 \sin(2t), \qquad q_{r2}(t) = 0.25 \sin(3t). \qquad (34)$$

Hence, $\omega_1 = 2$ [rad/s] and $\omega_2 = 3$ [rad/s] in the controller. The remaining parameter values of the controller are: $c_1 = c_2 = 5$, $s_1 = s_2 = 0.8$, $\mu_1 = \mu_2 = 0.1$. Then, by following (23), the control gains are chosen as: $k_{p1} = 35$, $k_{p2} = 115$, $k_{v1} = 12$, $k_{v2} = 30$.

The initial conditions of the robots are $q_{11} = -0.1$ [m], $q_{12} = 0$ [m], $q_{21} = -0.25$ [rad], $q_{22} = 0.25$ [rad]. The remaining initial conditions are zero. The experiment lasts 140 seconds and the obtained results are summarized in Figures 3 to 4.

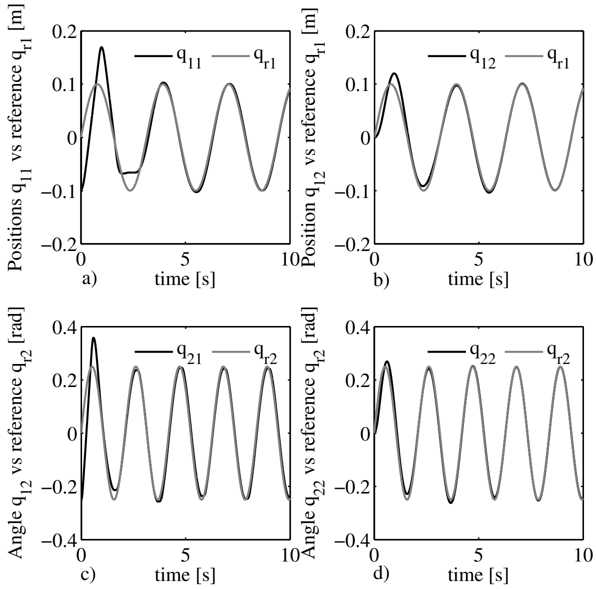

Fig. 3. Experimental results. The dofs of the robots synchronize in-phase with the desired trajectories. Figures a) and c): Real robot dofs vs reference trajectories. Figures b) and d): Virtual robot dofs vs reference trajectories.

After a short transient time, the robots *practically* synchronize [2] as depicted in Figure 3, where the tracking of the desired trajectories is evident. The tracking errors (not included here) are within the range ± 3 millimeters.

The control signals (32) applied to the robots, expressed in units of voltage, are depicted in Figure 4. From this figure it is clear that the actuators of the robots are far from saturation (the actuators tolerate a maximum input of ± 12 V).

6. EPILOGUE

In this contribution, we have made an attempt to show that Huygen's system of coupled clocks can be exploited for control applications. In fact, we have designed a controller by combining dynamical systems theory and control theory.

One of the advantages of our controller is that minimum interaction is needed to achieve synchronization and tracking of the desired reference $q_r(t)$. The reason behind this is that, after convergence, most of the terms in the controller vanish and the closed-loop behaves as a self-excited linear system. On the other hand, one of the drawbacks of the designed controller is that its performance is highly determined by how accurately the system dynamics is known, estimated, and/or reconstructed.

REFERENCES

Aihara, I., Kitahata, H., Yoshikawa, K., and Aihara, K. (2008). Mathematical model of frogs' calling behavior and its possible application to artificial life and robotics. *Artificial Life and Robotics*, 12, 29–32.

[2] The notion of practical synchronization is discussed in Blekhman et al. (1997).

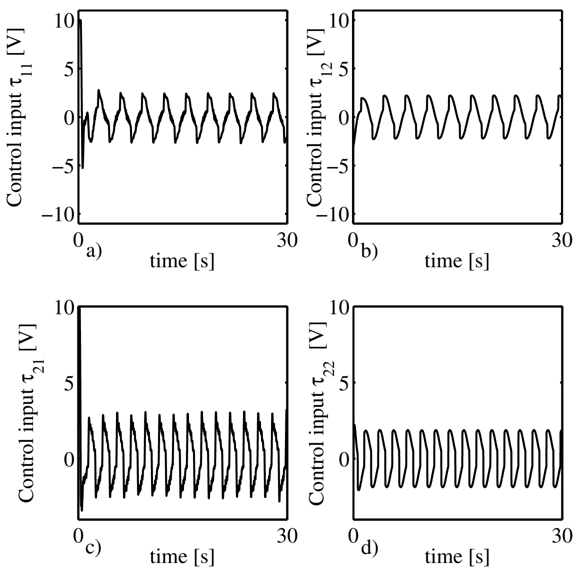

Fig. 4. Control inputs (in volts) to the robots. Figures a) and c): Inputs to real robot. Figures b) and d): Inputs to virtual robot.

Blekhman, I.I. (1971). *Synchronization of dynamic systems.* Nauka, Moscow.

Blekhman, I.I. (1988). *Synchronization in science and technology.* ASME Press, New York.

Blekhman, I.I., Fradkov, A. L., Nijmeijer, H., and Pogromsky, A. Yu. (1997). On self-synchronization and controlled synchronization. *Systems and Control Letters*, 31(5), 299–305.

Hoppensteadt, F.C. and Izhikevich, M. (2001). Synchronization of mems resonators and mechanical neurocomputing. *IEEE Transactions on Circuits and Systems I*, 48(2), 133–138.

Huygens, C. (1660). In M. Nijhoff (ed.), *Oeuvres completes de Christiaan Huygens*, volume 17, 156–189.

Levant, A. (2003). Higher-order sliding modes, differentiation and output-feedback control. *International Journal of Control*, 76, 924–941.

Nijmeijer, H. (2001). A dynamical control view on synchronization. *Physica D*, 154(3), 219–228.

Nijmeijer, H. and Rodriguez-Angeles, A. (2003). *Synchronization of Mechanical Systems.* World Scientific Publishing Company, Singapure.

Pena-Ramirez, J., Fey, R.H.B., and Nijmeijer, H. (2013). Synchronization of weakly nonlinear oscillators with Huygens' coupling. *Chaos: An Interdisciplinary Journal of Nonlinear Science*, 23, 033118.

Wang, C., Cao, M., and Xie, G. (2011). Anti-phase formation swimming for autonomous robotic fish. In *Proceedings of the 18th IFAC World Congress.* August 28 - September 2, Milano, Italy.

Appendix A. EXISTENCE AND STABILITY OF PERIODIC SOLUTIONS IN NONAUTONOMOUS SYSTEMS

Consider the nonautonomous system of equations

$$\dot{y}_s = \lambda_s y_s + \mu F_s(y_1, \ldots, y_l, \mu, \omega t), \qquad s = 1, \ldots, l, \quad \text{(A.1)}$$

where λ_s are the so-called characteristic exponents of system (A.1) when $\mu = 0$, and F_s are analytic and periodic functions of period $T = 2\pi/\omega$.

Assumption: The characteristic exponents of (A.1) can be classified as follows:

$$\lambda_s = i n_s \omega, \qquad s = 1, \ldots, k, \quad \text{(A.2)}$$

$$\lambda_s = -a_s \pm b_s, \qquad s = k+1, \ldots, l. \quad \text{(A.3)}$$

where $n_s \in \mathbb{Z}$, $a, b \in \mathbb{R}_+$.

Hence, for $\mu = 0$, system A.1 has the asymptotic solutions:

$$y_s^0 = \alpha_s e^{i n_s \omega t} \qquad s = 1, \ldots, k, \quad \text{(A.4)}$$

$$y_s^0 = 0 \qquad s = k+1, \ldots, l,$$

where α_s are constants determining the amplitude of the solution and are to be determined.

The following theorem, which is a particular case of a general theorem derived by Blekhman (1988), provides conditions for the existence and stability of periodic solutions in system (A.1). For the proof of the general Theorem, the reader is referred to Blekhman (1971).

Theorem 3. *Periodic solutions of the nonautonomous set of equations (A.1), which become periodic solutions (A.4) of the fundamental system, i.e. system (A.1) with $\mu = 0$, can correspond only to such values of constants $\alpha_1, \ldots, \alpha_k$, which satisfy equations*

$$P_s(\alpha_1, \ldots, \alpha_k) := \int_0^T F_s(y_1^0, \ldots, y_l^0, t) e^{-i n_s \omega t} dt = 0, \quad \text{(A.5)}$$

for $s = 1, \ldots, k$. If for certain set of constants $\alpha_1 = \alpha_1^*, \ldots, \alpha_k = \alpha_k^*$ which satisfy condition (A.5), the real part of all roots χ of the following characteristic equation are negative[3]

$$p(\chi) = det\left(\left.\frac{\partial Q}{\partial \alpha}\right|_{\alpha = \alpha_k} - \chi I \right) \quad \text{(A.6)}$$

then, for sufficiently small μ, this set of constants will correspond to a unique, analytically w.r.t μ asymptotically stable periodic solution of equation (A.1). If the real part of at least one root of equation (A.6) is positive, then the corresponding solution is unstable.

[3] $\left.\frac{\partial Q}{\partial \alpha}\right|_{\alpha=\alpha^*} = \left.\begin{bmatrix} \frac{\partial P_1}{\partial \alpha_1} & \cdots & \frac{\partial P_1}{\partial \alpha_k} \\ \vdots & \ddots & \vdots \\ \frac{\partial P_k}{\partial \alpha_1} & \cdot & \frac{\partial P_k}{\partial \alpha_k} \end{bmatrix}\right|_{\alpha_1 = \alpha_1^*, \ldots, \alpha_k = \alpha_k^*}$; $I \in \mathbb{R}^{k \times k}$ is the identity matrix.